

# Open System for Micro-Ultrasound

Weibao Qiu<sup>1</sup>, Hairong Zheng<sup>1</sup>, and Lei Sun<sup>2</sup>,

<sup>1</sup>Paul C. Lauterbur Research Center for Biomedical Imaging, Institute of Biomedical and Health Engineering,  
Shenzhen Institutes of Advanced Technology, Chinese Academy of Sciences, Shenzhen China

<sup>2</sup>Interdisciplinary Division of Biomedical Engineering, The Hong Kong Polytechnic University, Hong Kong, China  
lei.sun@polyu.edu.hk

**Abstract**—Micro-ultrasound is able to delineate small structures with fine spatial resolution on the order of several tens of microns. It is an invaluable imaging tool for many clinical and preclinical applications. This paper presents the development of an open system for various biomedical studies. The system design was based on field programmable gate array (FPGA) embedded in a printed circuit board to achieve flexible imaging applications. The major image processing algorithms were achieved by the novel field programmable technology for high speed and flexibility. Real-time imaging processing was achieved by fast processing algorithms and high speed data transfer interface. Extensive tests including hardware, algorithms, tissue mimicking phantom, and tissue specimen measurements were conducted to demonstrate good performance of the system. Multi-modality imaging was also facilitated by the developed open system.

**Keywords**—Micro-ultrasound, FPGA, PCB, programmable, real-time

## I. INTRODUCTION

High resolution, noninvasive imaging is always desired in preclinical research and clinical diagnosis. Among the available imaging modalities, micro-ultrasound has become more acceptable because of a good balance of spatial resolution, penetration depth, cost and safety. Fine anatomical structures can be visualized by this technique for clinical applications in ophthalmology, dermatology, and intravascular diseases [1]. Preclinical small animal model research has also been significantly propelled by micro-ultrasound such as tumor diagnosis, cardiac diseases, and biology [2].

Currently, a number of micro-ultrasound systems have been reported with different implementation, including single element transducer based system [3-4] and linear array transducer based systems [5-6]. Recently, micro-ultrasound has been combined with optical method such as optical coherence tomography (OCT) or fluorescence spectroscopy as a multi-modality imaging technique and demonstrated great potentials in biomedical studies [7]. Other advanced imaging techniques also take advantage of high-resolution micro-ultrasound and extended its biomedical investigations such as photoacoustic imaging, contrast enhanced imaging, coded excitation imaging, 3-D imaging, and elastography imaging. Each study is unique in nature, and requires different utilization of the micro-

ultrasound system. System with fixed specifications, such as transducer characteristics, data acquisition strategy, signal processing method, and image display approach, does not satisfy extensive preclinical study requirements. Researchers need a highly flexible device to best suit their specific investigations. In addition, access to the raw experimental data is also important to scientific discovery. Therefore an open and flexible micro-ultrasound system allowing users/researchers to customize for individual biomedical study is necessary.

This paper describes the development of an open micro-ultrasound system with high flexibility and compactness to satisfy various biomedical investigations. An FPGA serves as the core processor and replaces hardware circuitry with high processing speed and programmability. Moreover, low noise and high speed analog electronics were used to achieve a high signal-to-noise ratio (SNR) and a high sensitivity. A high speed PCI Express (PCIE) interface was incorporated in this system as a high speed data transmission interface for image data or raw RF data transfer to a computer through direct memory access operation. We demonstrated that both B-mode imaging and directional PW Doppler can be realized on this system. In addition, this system was also capable for intravascular ultrasound (IVUS) imaging. Finally, phantom and in vivo measurements were conducted to demonstrate the system performance.

## II. MATERIALS AND METHODS

The block diagram of the designed open system is shown in Fig. 1. Two main parts are involved: pulse generator and imaging receiver. A pulse generator generates high voltage short pulse to excite the transducer at desired frequency and spectrum specifications. An FPGA-based high speed digital imaging receiver is developed to process the ultrasound echo signal for programmability and flexibility. The receiver incorporates the front-end electronics such as amplifier, filter, and analog-to-digital converter (ADC), FPGA microprocessor, and PCIE interface. The system is designed on electronic components and PCB for a compact implementation. A personal computer is employed for image display and data storage for further investigations. A miniaturized ultrasonic transducer was employed for ultrasound signal generation and echo receiving. A customized motor was fabricated to drive the transducer to acquire a cross-

sectional view of target vessels. A personal computer is employed for image display and data storage for further investigations. Graphical user interface software is programmed in Visual C++ to process and display the real-time ultrasound images.

### A. Pulse Generator

The designed pulse generator for this open system incorporated a bipolar pulse generation scheme. A programmable FPGA component (Cyclone III, EP3C16F484C6N, Altera Corporation, San Jose, CA) was employed to control the timing and spectrum characteristics of the high voltage short pulse. Therefore, the pulse generator can be easily adjusted to support transducers with different center frequency as well as to match with the spectrum of individual transducer to acquire the optimized performance. Two metal-oxide-semiconductor field effect transistor (MOSFET) drivers (EL7158, Intersil Corporation, Milpitas, CA) were employed to accomplish the voltage level shift and high current output to excite the high-speed MOSFET pair (TC6320, Supertex Inc., Sunnyvale, CA). The MOSFET pair could offer more than 150Vpp breakdown voltages and a 2A output peak current, which made it suitable to produce a high-voltage pulse for micro-ultrasound. The T/R switch was achieved by the crossed diode bridge to block the reflected signal from the transducer. Finally, the pulse generator performance was evaluated by a digital oscilloscope (LeCroy wavepro 715Zi, LeCroy Corp., Chestnut Ridge, NY) with a series of attenuators (Mini-Circuits, Brooklyn, NY).

### B. Imaging Receiver

The echo signal received from the transducer is sent to the receiver for imaging processing. A low noise preamplifier (SMA231, Tyco Electronics Co., Berwyn, PA) was used as the first stage to achieve a good SNR, followed by a second stage amplifier (THS4509, Texas Instruments Inc., Dallas, TX) to achieve adequate amplification gain. Specific amplifier for high frequency applications may also be possible for the small signal amplification. A high speed, 11 bits ADC (ADS5517, Texas Instruments Inc., Dallas, TX) with a maximum sampling rate of 200 mega-samples per second (MSPS) was utilized for signal digitization. After the digitization, the signal was transferred to FPGA through low voltage differential signaling (LVDS) bus. A high performance FPGA (Stratix II EP2S60F672C5, Altera Corporation, San Jose, CA) was employed for programmable signal/image processing and high speed data transfer. It could achieve various programmable algorithms such as band-pass filter, Hilbert transform, envelop detection and digital scan conversion. A 128M bits synchronous dynamic random access memory (SDRAM) (MT48LC8M16A2, Micron Technology Inc., Boise, ID) was configured to FPGA for temporary data storage. Finally, the processed images or raw RF data were transferred to a computer through a PCIE interface component (PEX8311, PLX Technology

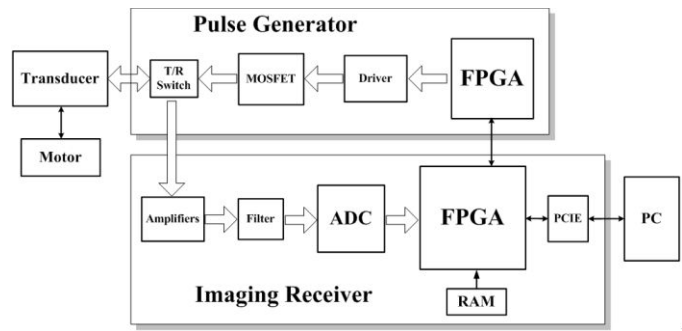


Figure 1. The block diagram of the real-time annular array imaging platform for micro-ultrasound.

Inc, Sunnyvale, CA) for displaying, storage or post-processing.

### C. Imaging Algorithms

As a field programmable microprocessor, the FPGA can achieve various functionalities traditionally realized

by hardware circuitry. Moreover, the functions can easily be changed or modified by reprogramming the FPGA without change of hardware. Thus, the FPGA technology can significantly improve the system flexibility and diversity by programmable and reconfigurable algorithms. Fig. 2 shows a representative structure of image processing algorithms for real-time micro-ultrasound imaging. The entire processing algorithms could be easily reprogrammed according to different applications. A double data rate LVDS buffer is used to decode the digitized ultrasound echo data through high speed ADC. Both the rising and falling edges of clock are employed for data transferring to achieve high data throughput. A band-pass filter (BPF) based on finite impulse response (FIR) structure is used to remove noise out of spectrum of interests. The coefficient of the BPF is reconfigurable for individual transducers with different center frequency and bandwidth. The filtered signal is then sent to the envelope detector to achieve envelope extraction by Hilbert transform algorithm. The acquired envelope data are then undergone digital scan conversion and logarithmic compression for coordination conversion and data compression, respectively. A flexible scan converter based on linear interpolation is employed for fast and accurate processing. Finally, image data are sent to a personal computer through PCIE interface for display and storage. A SDRAM controller is employed to buffer data with external SDRAM for flexible digital scan conversion and logarithmic compression.

## III. RESULTS

The photographs of the open IVUS system prototypes are shown in Fig. 3. Fig. 3(a) shows the pulse generator in an eight-layer PCB. It includes the FPGA, MOSFETs, and

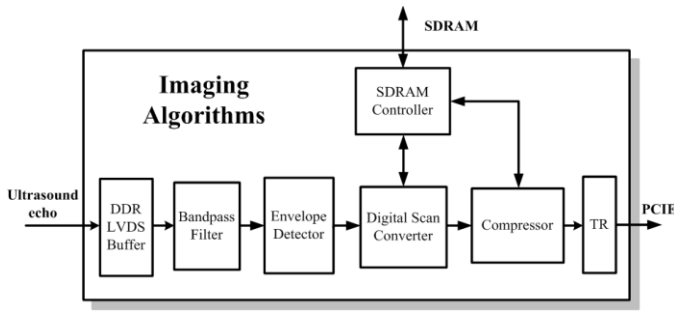


Figure 2. The algorithms implemented in FPGA for real-time micro-ultrasound imaging.

MOSFET drivers. Fig. 3(b) shows the digital imaging receiver. It is also an eight-layer PCB design incorporating state-of-the-art electronics such as low noise front-end amplifiers, ADCs, FPGA, and high speed PCIE interface. The electronics are soldered on the PCB for compactness. High speed PCIE interface was used for real-time data acquisition.

#### A. System Evaluation

The highest amplitude of bipolar pulse was 160Vpp with adjustable center frequency and bandwidth. The maximum gain of the front-end electronics is 47dB with good linearity at a maximum fluctuation of less than  $\pm 1.2$ dB between 10MHz and 90MHz. The noise floor level of the system receiver is less than 25 $\mu$ V. Given the input range of the high speed ADC (2Vpp), the system can allow a 51dB dynamic range at 35MHz center frequency.

The software-based band pass filter (BPF) was programmed in the FPGA to further remove the noise and improve the signal SNR. Quantitative analysis showed that approximately 4.8dB SNR improvement was achieved after applying the BPF, which increased the system dynamic range to 55.8dB. The algorithms currently in FPGA occupy small amount FPGA resources. There are significant amount of resources left to support other techniques such as spectrum analysis imaging etc. Much more complicated signal processing may be implemented to acquire more useful information.

The algorithmic scheme implemented in the FPGA can achieve high speed imaging by pipe-line signal processing. The data transferring speed was higher than 150MByte/s in the case of PCIE interface. At the image size of 512 $\times$ 512 pixels, the frame rate can be higher than 200 images per second. Current frame rate is limited by the mechanical motor, and it can be significantly improved if a faster mechanical motor is used.

#### B. B-mode Imaging

A tissue mimicking phantom was fabricated to test the image quality of the open system. The phantom consists of a mixture of deionized water, high-grade agarose, preservative, propylene glycol, filtered bovine milk, and

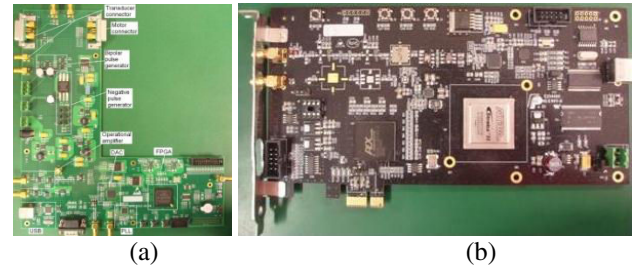


Figure 3. Photos of the pulse generator (a), and echo receiver (b) for the designed open system.

glass-bead to generate tissue mimicking attenuation and backscattering. Anechoic spheres were fabricated separately and dispersed in the phantom to test the system resolution [39]. The size of the anechoic spheres was in the range of 180 $\mu$ m-280 $\mu$ m controlled by a dedicated sieve (Fisherbrand sieves, Fisher Scientific, Pittsburgh, PA). The black circular dots in the images are the anechoic spheres. The measured diameter of the spheres in the images is approximately 180 $\mu$ m, which is in good agreement with the actual sphere size. The transducer for this experiment was a 40 MHz transducer with a focal length of 6.3 mm. The -6 dB bandwidth was 108%.

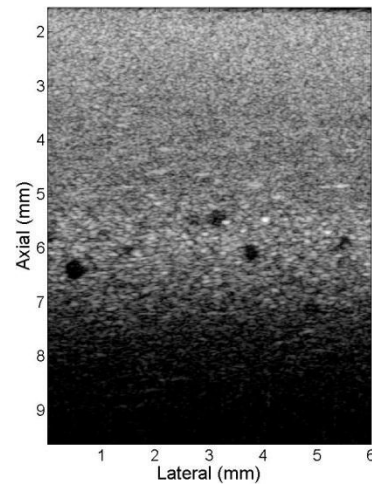


Figure 4. Image of tissue phantom with anechoic spheres.

#### C. Flow Imaging

Fig. 5 shows an in vivo spectrogram acquired from a vein at the back of a human hand. A needle transducer (42.5MHz) was placed close to the vein coupled by ultrasound gel with the angle of approximately 72 degree. A seven-cycle 40Vpp sinusoidal pulse was generated with a pulse repetition frequency of 1.95 kHz. The blood actually flowing away from the transducer confirmed the negative velocity profile. The cyclic pattern of the spectrogram correlated well to the heart beat of the subject. The heart rate was 80 beats/min measured from the spectrogram agreed with the heart rate of 78 beats/min of the human subject.

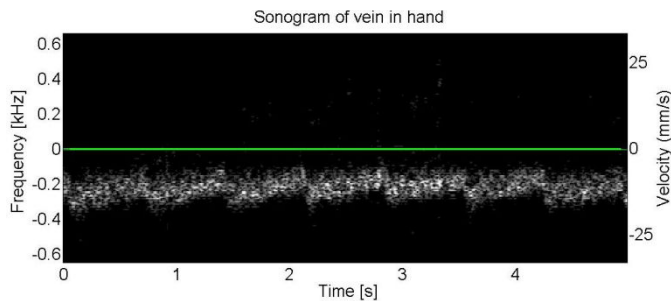


Figure 5. Pulsed-wave Doppler waveform of a vein in the back of a human hand.

#### D. Intravascular Imaging

The designed open system supports various applications for micro-ultrasound techniques. Intravascular ultrasound imaging was also achieved by replacing the transducer with IVUS transducer. The motor was also changed with a rotary motor. In vitro coronary artery specimen was used for system evaluation. The ultrasound image of specimen is shown in Fig. 6(a). Different layers of the artery can be clearly identified in the ultrasound image. The result from a multi-modality imaging combining IVUS and photoacoustics is shown in Fig. 6(b). An actively Q-switched pulsed laser (Explorer 532 Laser System, Spectra-Physics, Santa Clara, CA) operating at 532 nm wavelength generated very short laser pulses with 240 $\mu$ J energy. Ultrasound imaging was launched after the acquisition of photoacoustic signal. The echo intensity of ultrasound imaging slightly increases in bottom right corner of the tissue. This difference can be clearly visualized in photoacoustic image which may indicate the change of tissue composition. Combined image shows the complementary nature of ultrasound imaging and photoacoustic imaging that could be useful for the diagnosis of intravascular diseases. This in vitro experimental result clearly demonstrated the capability and flexibility of the proposed open system.

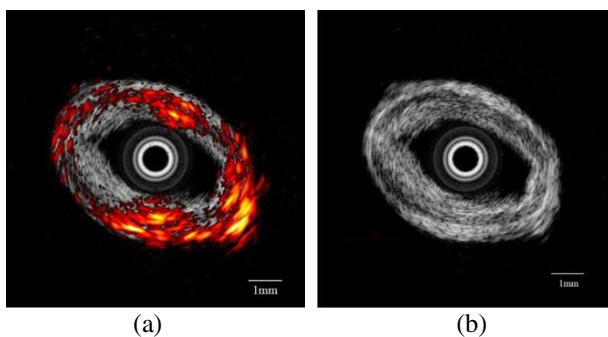


Figure 6. *In vitro* imaging of human coronary artery. (a) IVUS image. (b) Combined image of IVUS and photoacoustics.

#### IV. CONCLUSION

In this paper, a programmable open system for real-time micro-ultrasound was developed and evaluated based on a high-speed FPGA. It was implemented in a compact and cost-effective PCB scheme. This open system demonstrated a high image quality with a good spatial resolution for preclinical small animal imaging. The flexible and programmable design makes the open system suitable for various biomedical studies.

#### ACKNOWLEDGMENT

The financial support from the Hong Kong Research Grant Council (RGC) General Research Fund (GRF) (PolyU 5301/09E), and The Hong Kong Polytechnic University (A-PJ84) are gratefully acknowledged.

#### REFERENCES

- [1] F. S. Foster, C. J. Pavlin, K. A. Harasiewicz, D. A. Christopher, and D. H. Turnbull, "Advances in ultrasound biomicroscopy," *Ultrasound Med. Biol.*, vol. 26, no. 1, pp. 1-27, 2000.
- [2] F. S. Foster, J. Hossack, and S. L. Adamson, "Micro-ultrasound for preclinical imaging," *Interface Focus*, vol. 1 no. 4, pp. 576-601, 2011.
- [3] L. Sun, C. Lien, X. Xu, and K. K. Shung, "In vivo cardiac imaging of adult zebrafish using high frequency ultrasound (45-75 MHz)," *Ultrasound Med. Biol.*, vol. 34, No. 1, pp. 31-39, 2008.
- [4] W. Qiu, Y. Yu, F. K. Tsang, and L. Sun, "A multi-functional, reconfigurable pulse generator for high frequency ultrasound imaging," *IEEE Trans. Ultrason. Ferroelectr. Freq. Control*, vol. 59, no. 7, pp. 1432-1442, 2012.
- [5] C. Hu, L. Zhang, J. M. Cannata, J. Yen, and K. K. Shung, "Development of a 64 channel ultrasonic high frequency linear array imaging system," *Ultrasonics*, vol. 51, no. 8, pp. 953-959, 2011.
- [6] W. Qiu, Y. Yu, H. R. Chabok, C. Liu, F. K. Tsang, Q. Zhou, K. K. Shung, H. Zheng, and L. Sun, "A flexible annular array imaging platform for micro-ultrasound," *IEEE Trans. Ultrason. Ferroelectr. Freq. Control*, vol. 60, no. 1, 2013.
- [7] H. C. Yang, J. Yin, C. Hu, J. Cannata, Q. Zhou, J. Zhang, Z. Chen, and K. K. Shung, "A dual-modality probe utilizing intravascular ultrasound and optical coherence tomography for intravascular imaging applications," *IEEE Trans. Ultrason. Ferroelectr. Freq. Control*, vol. 57, no. 12, pp. 2839-2843, 2010.
- [8] E. L. Madsen, G. R. Frank, M. M. McCormick, M. E. Deaner, and T. A. Stiles, "Anechoic sphere phantoms for estimating 3-D resolution of very-high-frequency ultrasound scanners," *IEEE Trans. Ultrason. Ferroelectr. Freq. Control*, vol. 57, no. 10, pp. 2284-2292, 2010.